

Crack identification in two-dimensional unilateral contact mechanics with the boundary element method

C. Alessandri, V. Mallardo

100

Abstract The identification of a unilateral frictionless crack is performed in nonlinear elastostatics by using boundary measurements for given static loadings. The procedure proposed takes into account the possibility of a partial or total closure of the crack during the identification process; that makes the present formulation more complex than others referred to permanently open cracks. The Linear Complementarity Problem (LCP), which provides at each step contact tractions and relative displacements along the crack, is discretised by means of the Dual Boundary Element Method (DBEM) and solved explicitly by Lemke's algorithm. The identification procedure is based on a first-order nonlinear optimisation technique in which the gradients of the cost function are obtained by solving again a LCP with a considerably reduced number of variables. Some numerical examples show the applicability of the method.

1

Introduction

In this paper an inverse problem in nonlinear elastostatics is considered: it concerns the identification of cracks under frictionless unilateral contact conditions on the basis of boundary measurements related to prescribed static loadings. As a matter of fact, the problem of identifying an even partially closed crack has been barely tackled in the literature, where the identification of cracks which never close or of inclusions in bilateral contact with the matrix has been more frequently discussed. Nevertheless, the tight connection between nonlinear structural response and crack closure has been widely acknowledged. It is worth noting that the closure of a crack, either totally or partially, is strictly dependent on the forces applied; therefore, different loading cases are considered in testing the proposed identification procedure.

Here, the direct static frictionless unilateral contact problem for a linear elastic two-dimensional body with an internal crack is treated numerically by the DBEM. The arising variational inequality problem leads, after the discretisation performed with linear boundary elements based on collocations, to a non-symmetric LCP which is solved by Lemke's complementarity pivoting technique.

The choice of boundary element methods is generally acknowledged as more appropriate for this kind of inverse problems since only a small number of data, the ones concerning the crack surfaces, need to be stored and adapted along the required repetitive procedure.

For more detailed informations on variational inequality problems in unilateral contact mechanics and their numerical solution with boundary element methods, the reader is referred to Alliney et al. (1990), Antes and Panagiotopoulos (1992), Simunovic and Saigal (1992, 1994).

An error function is introduced into the iterative procedure of the inverse problem as a measure of the difference between the computed displacements and the ones observed at some sensor points on the boundary. This function is then minimised in order to give the actual position and shape of the flaw.

The minimisation is performed by using a first-order nonlinear unconstrained optimisation technique in which the error function gradient is computed by the implicit differentiation method.

For the presence of the unilateral constraints, the structural analysis response is a nonconvex and nondifferentiable function of the crack parameters; the sensitivity of this response can be calculated only along given directions and the sensitivity matrix must be interpreted in a generalised sense. The fundamental aspects of the sensitivity analysis for a continuum problem governed by boundary variational inequalities are presented in Alessandri and Tralli (1995). To the author's knowledge, no general algorithm exists at present which guarantees the convergence to a global solution of the problem and allows to overcome the difficulties depending on the ill-posedness of the inverse problem, the lack of convexity and differentiability of the cost function.

In this paper a two-dimensional specimen containing an unknown crack is considered. The crack is idealised by a certain number of parameters, e.g. the co-ordinates of its extreme points. It is assumed that certain boundary displacements can be measured for various external loadings. The direct mechanical problem is solved numerically by the previously outlined DBEM-LCP method, while the general identification step is treated by a first-order

Received 23 November 1998

C. Alessandri (✉), V. Mallardo
Dipartimento di Architettura Università degli Studi di Ferrara
Via Quartieri, 8 44100 Ferrara, Italy

This work is part of a research project sponsored by the "Ministero dell'Università e della Ricerca Scientifica e Tecnologica" under a grant MURST 40%. The authors are grateful to Prof. A. Tralli for his helpful support in developing this research.

non-linear optimisation technique. The inverse problem consists in the determination of the parameters which define the unknown crack (design variables $\mathbf{z} = (z_1, \dots, z_m, \dots, z_M)$), and it can be formulated as a minimisation problem with respect to the difference between the measured displacements and the computed ones.

Most published work concerns crack and cavity identification in fields governed by Laplace equation (Friedman and Vogelius 1989; Nishimura and Kobayashi 1991; Santosa and Vogelius 1991; Zeng and Saigal 1992), elastostatic equation (Tanaka and Masuda 1986; Schnur and Zabarar 1992; Bezerra and Saigal 1993; Kassab et al. 1994; Mellings and Aliabadi 1995; Tosaka et al. 1995), Helmholtz and elastodynamic equations (Tanaka et al. 1992; Kobayashi 1994; Nishimura and Kobayashi 1995; Burczyński et al. 1997; Mallardo and Aliabadi 1998). In all the papers dealing with elastostatics and elastodynamics the crack is treated as bilateral, thus the numerical results are not corresponding to the actual physical behaviour.

A novel contribution of Cruse et al. (1999) introduces a special two-dimensional Green's function for electromagnetic problems in the presence of a crack. Such a function, corresponding to zero flux across the crack, is validated by comparisons both with exact solution and with experimental results. The work does not take into account the electrical conductivity caused by a partial closure of the crack.

The work of Stavroulakis and Antes (1997) can be considered as a first attempt to solve the unilateral frictionless crack identification problem in elasticity: a multiregion boundary element formulation is coupled to a neural network based optimisation technique in order to obtain the actual shape and position of the internal crack. This procedure presents three disadvantages if compared to the formulation proposed in this work: a higher number of unknowns, the need of a more complicated procedure to update the discretisation at each step and a less effective minimisation software. On the other hand, however, the use of neural networks allows to bypass numerical problems connected with the occurrence of local minima.

On the basis of such considerations, in Sect. 2 the direct problem is solved: a brief description of the discretised LCP referred to unilateral contact is followed by the governing integral equations within the DBEM and by the numerical treatment of the singular and hypersingular integrals involved. In Sect. 3 the implicit differentiation method applied to the sensitivity analysis is presented: the derivative forms of the linear complementarity relations and of the boundary integral equations are obtained with respect to the design variables in order to compute the sensitivities required by the optimisation procedure. This section ends up with the evaluation of the arising singular and hypersingular integrals. In Sect. 4 the error function and its gradient are presented. Finally, in Sect. 5 two simple but meaningful examples of frictionless unilateral crack identification are presented and discussed in detail in order to show the applicability of the proposed technique.

2

Direct problem

Let us consider (Fig. 1) a linear elastic body B occupying a bounded domain $\Omega \subset R^2$ with a sufficiently regular

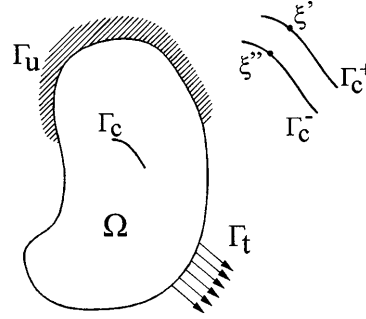


Fig. 1. Geometry of the problem

boundary $\Gamma_e = \Gamma_t \cup \Gamma_u$ and with an internal frictionless unilateral crack $\Gamma_c = \Gamma_c^+ \cup \Gamma_c^-$. An external force vector \mathbf{t} is assigned over Γ_t , while the prescribed displacements \mathbf{u} on Γ_u , the body force \mathbf{b} and any initial strain field are assumed equal to zero for simplicity.

The undeformed crack lines Γ_c^+ and Γ_c^- are assumed to be sufficiently regular, i.e. they are given by sufficiently smooth functions.

Furthermore, kinematic relations are considered within the “small displacements and small deformations theory” which allows to assume no major changes in the contact zone during the deformation process.

The DBEM and the LCP are used to provide displacements and tractions both on the external boundary and along the internal crack.

If $\mathbf{u}_{\Gamma_e}^q$ collects the displacements on the external boundary Γ_e due to the applied load \mathbf{t} obtained by assuming the internal crack as bilateral, the actual displacements \mathbf{u}_{Γ_c} on the same boundary can be stated as

$$\mathbf{u}_{\Gamma_c} = \mathbf{u}_{\Gamma_e}^q + \mathbf{K}\mathbf{p} \quad (1)$$

where \mathbf{p} collects the contact crack pressures and \mathbf{K} is a suitable influence matrix.

The DBEM is used to obtain vector $\mathbf{u}_{\Gamma_e}^q$ and matrix \mathbf{K} , while the LCP is solved to get the vector \mathbf{p} .

2.1

Linear complementarity problem

Let us consider a two-dimensional cracked body discretised with NE linear boundary elements. Each element has two nodes and it is continuous on the external boundary, discontinuous along the crack. The latter condition is necessary to guarantee the existence of the Hadamard principal value integral involved in the DBEM.

In order to solve the cracked body subjected to an external load, it is necessary to solve the following LCP

$$\mathbf{w} = \mathbf{w}_q + \mathbf{V}\mathbf{p} \geq 0 \quad (2a)$$

$$\mathbf{p} \geq 0 \quad \mathbf{w}^T \mathbf{p} = 0 \quad (2b)$$

where \mathbf{w} is the vector of the actual relative normal displacements of the crack nodes, \mathbf{w}_q collects the relative normal displacements of such nodes when loads and constraints are applied on the external boundary and zero tractions are imposed on the crack nodes, \mathbf{V} is an influence matrix the j th column of which contains the relative normal displacements at the crack nodes obtained by

imposing a unit normal pressure at nodes j^+ and j^- and known constraints on the external boundary nodes.

If NC is the number of the crack nodes, \mathbf{w}_q and \mathbf{V} are both evaluated by applying NC + 1 times the DBEM.

2.2

Single region boundary element formulation

The basic boundary integral equations are expressed in terms of displacements \mathbf{u} and tractions \mathbf{t} , i.e.

$$c_{ij}(\xi)u_j(\xi) + \int_{\Gamma} T_{ij}(\xi, \mathbf{x})u_j(\mathbf{x})d\Gamma(\mathbf{x}) = \int_{\Gamma} U_{ij}(\xi, \mathbf{x})t_j(\mathbf{x})d\Gamma(\mathbf{x}) \quad (3)$$

$$\frac{1}{2}u_i(\xi') + \frac{1}{2}u_i(\xi'') + \int_{\Gamma} T_{ij}(\xi', \mathbf{x})u_j(\mathbf{x})d\Gamma(\mathbf{x}) = \int_{\Gamma} U_{ij}(\xi', \mathbf{x})t_j(\mathbf{x})d\Gamma(\mathbf{x}) \quad (4)$$

$$\frac{1}{2}t_i(\xi'') - \frac{1}{2}t_i(\xi') + n_j(\xi'') \int_{\Gamma} S_{kij}(\xi'', \mathbf{x})u_k(\mathbf{x})d\Gamma(\mathbf{x}) = n_j(\xi'') \int_{\Gamma} D_{kij}(\xi'', \mathbf{x})t_k(\mathbf{x})d\Gamma(\mathbf{x}) \quad (5)$$

where (see Fig. 1) $\Gamma = \Gamma_e \cup \Gamma_c$, $\xi \in \Gamma_e$, $\xi' \in \Gamma_c^+$, $\xi'' \in \Gamma_c^-$, $\mathbf{x} \in \Gamma$ are position vectors, \int and \int stand for the Cauchy principal value integral and for the Hadamard principal value integral respectively, U_{ij} , T_{ij} and D_{kij} , S_{kij} are the fundamental solutions and combination of their derivatives respectively (Hong and Chen 1988; Brebbia and Dominguez 1992).

Equations (4) and (5) and their numerical treatment have been tackled by various authors (Guiggiani and Casalini 1987; Guiggiani et al. 1992; Liu et al. 1993; Martin et al. 1998; Liu 1998). Discussion of these equations is reported in Appendix.

The discretisation performed with continuous and discontinuous linear elements characterised by shape functions $M^n(\zeta)$ and Jacobian $J^l(\zeta)$, with ζ the local dimensionless variable, leads to the following boundary integral equations

$$c_{ij}(\bar{\xi})u_j(\bar{\xi}) + \sum_{l=1}^{EL} \sum_{n=1}^2 u_j^n \int_{-1}^{+1} T_{ij}(\bar{\xi}, \mathbf{x}(\zeta))M^n(\zeta)J^l(\zeta)d\zeta = \sum_{l=1}^{EL} \sum_{n=1}^2 t_j^n \int_{-1}^{+1} U_{ij}(\bar{\xi}, \mathbf{x}(\zeta))M^n(\zeta)J^l(\zeta)d\zeta \quad \text{for } \bar{\xi} \in \Gamma_e \quad (6)$$

$$\frac{1}{2}u_i(\bar{\xi}') + \frac{1}{2}u_i(\bar{\xi}'') + \sum_{l=1}^{EL} \sum_{n=1}^2 u_j^n \int_{-1}^{+1} T_{ij}(\bar{\xi}', \mathbf{x}(\zeta))M^n(\zeta)J^l(\zeta)d\zeta = \sum_{l=1}^{EL} \sum_{n=1}^2 t_j^n \int_{-1}^{+1} U_{ij}(\bar{\xi}', \mathbf{x}(\zeta))M^n(\zeta)J^l(\zeta)d\zeta \quad \text{for } \bar{\xi}' \in \Gamma_c^- \quad (7)$$

$$\frac{1}{2}t_i(\bar{\xi}'') - \frac{1}{2}t_i(\bar{\xi}') + n_j(\bar{\xi}'') \sum_{l=1}^{EL} \sum_{n=1}^2 u_k^n \int_{-1}^{+1} S_{kij}(\bar{\xi}'', \mathbf{x}(\zeta))M^n(\zeta)J^l(\zeta)d\zeta = n_j(\bar{\xi}'') \sum_{l=1}^{EL} \sum_{n=1}^2 t_k^n \int_{-1}^{+1} D_{kij}(\bar{\xi}'', \mathbf{x}(\zeta))M^n(\zeta)J^l(\zeta)d\zeta \quad \text{for } \bar{\xi}'' \in \Gamma_c^- \quad (8)$$

where $\bar{\xi}$, $\bar{\xi}'$, $\bar{\xi}''$ are the position vectors of the source nodes.

These equations, in a usual matrix form, can be stated as

$$\begin{bmatrix} \mathbf{H}_{\Gamma_e\Gamma_e} & \mathbf{H}_{\Gamma_e\Gamma_c^+} & \mathbf{H}_{\Gamma_e\Gamma_c^-} \\ \mathbf{H}_{\Gamma_c^+\Gamma_e} & \mathbf{H}_{\Gamma_c^+\Gamma_c^+} & \mathbf{H}_{\Gamma_c^+\Gamma_c^-} \\ \mathbf{H}_{\Gamma_c^-\Gamma_e} & \mathbf{H}_{\Gamma_c^-\Gamma_c^+} & \mathbf{H}_{\Gamma_c^-\Gamma_c^-} \end{bmatrix} \begin{bmatrix} \mathbf{u}_{\Gamma_e} \\ \mathbf{u}_{\Gamma_c^+} \\ \mathbf{u}_{\Gamma_c^-} \end{bmatrix} = \begin{bmatrix} \mathbf{G}_{\Gamma_e\Gamma_e} & \mathbf{G}_{\Gamma_e\Gamma_c^+} & \mathbf{G}_{\Gamma_e\Gamma_c^-} \\ \mathbf{G}_{\Gamma_c^+\Gamma_e} & \mathbf{G}_{\Gamma_c^+\Gamma_c^+} & \mathbf{G}_{\Gamma_c^+\Gamma_c^-} \\ \mathbf{G}_{\Gamma_c^-\Gamma_e} & \mathbf{G}_{\Gamma_c^-\Gamma_c^+} & \mathbf{G}_{\Gamma_c^-\Gamma_c^-} \end{bmatrix} \begin{bmatrix} \mathbf{t}_{\Gamma_e} \\ \mathbf{t}_{\Gamma_c^+} \\ \mathbf{t}_{\Gamma_c^-} \end{bmatrix} \quad (9)$$

where the first subscript of every sub-matrix gives the position of the source node, the second one the position of the integration element and the subscript of every vector gives the position of the node to which the vector is related. The singular term in (6) is evaluated by the rigid body condition (Brebbia and Dominguez 1992), whereas the other singular and hyper-singular terms in (7) and (8) are calculated analytically.

After applying the boundary conditions and interchanging accordingly columns of \mathbf{H} and \mathbf{G} , matrix equation (7) becomes

$$\mathbf{Ax} = \mathbf{b} \quad (10)$$

After obtaining the solution of the system of equations (10), it is possible to point out the relative normal displacements $\Delta\mathbf{u}_{\Gamma_c}^n$ of the crack nodes by performing a local co-ordinate transformation.

Although any standard linear algebraic routine can be used to solve the above system, the one applied here is based on the LU decomposition. Such a choice is due to the repeated computations, with only forward and backward substitution at each step, required in the sensitivity analysis which will be presented in Sect. 3.

2.2.1

Analytic integration

As mentioned earlier, on the crack boundary, analytical integration of the weakly-singular and singular integrals is carried out. These integrals arise from U_{ij} , T_{ij} terms in the displacement equation (7) and from D_{kij} , S_{kij} terms in the traction equation (8) when the field point is on the crack boundary.

With reference to a flat, discontinuous element, the weakly-singular integral is given as

$$\int_{-1}^{+1} U_{ij}(\bar{\xi}, \mathbf{x}(\zeta))M^n(\zeta)J^l(\zeta)d\zeta = \frac{3}{32} \frac{L}{\pi\mu(1-v)} \left[(3-4\nu)WI\delta_{ij} + g_{ij}^n \right] \quad (11)$$

$$WI = \int_{-1}^1 \ln\left(\frac{4}{3L|\zeta - \zeta'|}\right) M^n(\zeta) d\zeta \quad (12)$$

where δ_{ij} is the delta Kronecker, ζ' is the local dimensionless co-ordinate of the source node, L the distance between the two nodes of the element, μ and ν the second Lamé constant and Poisson's ratio respectively, $g_{11}^n = n_2^2$, $g_{12}^n = g_{21}^n = -n_1 n_2$, $g_{22}^n = n_1^2$ with (n_1, n_2) the components of the outward normal to the element.

The singular integrals are given as

$$\begin{aligned} & \int_{-1}^1 T_{ij}(\bar{\xi}', \mathbf{x}(\zeta)) M^n(\zeta) J^l(\zeta) d\zeta \\ &= \frac{1-2\nu}{4\pi(1-\nu)} h_{ij}^n \int_{-1}^1 \frac{M^n(\zeta)}{\zeta - \zeta'} d\zeta \end{aligned} \quad (13)$$

$$\begin{aligned} & \int_{-1}^1 D_{kij}(\bar{\xi}'', \mathbf{x}(\zeta)) M^n(\zeta) J^l(\zeta) d\zeta \\ &= \frac{1}{4\pi(1-\nu)} \bar{g}_{kij}^n \int_{-1}^1 \frac{M^n(\zeta)}{\zeta - \zeta'} d\zeta \end{aligned} \quad (14)$$

$$\begin{aligned} & \int_{-1}^1 S_{kij}(\bar{\xi}'', \mathbf{x}(\zeta)) M^n(\zeta) J^l(\zeta) d\zeta \\ &= \frac{E}{3\pi l(1-\nu^2)} \bar{h}_{kij}^n \int_{-1}^1 \frac{M^n(\zeta)}{(\zeta - \zeta')^2} d\zeta \end{aligned} \quad (15)$$

where

$$\mathbf{h}^n = \begin{pmatrix} 0 & -1 \\ 1 & 0 \end{pmatrix} \quad (16)$$

$$\begin{aligned} \bar{\mathbf{g}}^n &= \begin{pmatrix} 111 & 112 \\ 122 & 211 \\ 212 & 222 \end{pmatrix} \\ &= \begin{pmatrix} (2\nu-1)n_2 - 2n_2^3 & (1-2\nu)n_1 + 2n_1 n_2^2 \\ (1-2\nu)n_2 - 2n_1^2 n_2 & 2n_1 n_2^2 - (1-2\nu)n_1 \\ (2\nu-1)n_2 - 2n_1^2 n_2 & (1-2\nu)n_1 + 2n_1^3 \end{pmatrix} \end{aligned} \quad (17)$$

$$\bar{\mathbf{h}}^n = \begin{pmatrix} n_1(2n_2^2 + 1) & n_2(1 - 2n_1^2) \\ n_1(2n_1^2 - 1) & n_2(1 - 2n_2^2) \\ n_1(1 - 2n_2^2) & n_2(2n_1^2 + 1) \end{pmatrix} \quad (18)$$

E is the Young modulus, $\bar{g}_{121}^n = \bar{g}_{112}^n$, $\bar{g}_{221}^n = \bar{g}_{212}^n$ and the same for the \bar{h}_{kij}^n coefficients.

The integrals involved in Eq. (14) and (15) can be computed analytically following Guiggiani and Casalini (1987) and Guiggiani et al. (1992). The right hand side term of Eq. (15), in particular, can be easily evaluated because the arising unbounded terms cancel out.

It is worth noting that the integration of U_{ij} and D_{kij} terms is not required if the crack is bilateral since it is usually assumed to be traction free. In the proposed procedure, this integration is necessary to obtain the \mathbf{V} and \mathbf{K} matrices.

3

Design sensitivity analysis

In this section the computation of the design sensitivities is carried out. Design sensitivities represent the variations

of external displacements and tractions in dependence of changes in design parameters. These are necessary in order to implement the identification numerical procedure by using any first-order optimisation technique.

In this work an implicit differentiation design sensitivity analysis is presented. The procedure uses the derivative form of the discretised integral equations (6)–(8) and the linear complementarity technique in order to obtain the derivatives of displacements $\mathbf{u}_{\Gamma_e, m}$ on the external boundary with respect to a design variable.

Design sensitivities $\mathbf{u}_{\Gamma_e, m}$ can be computed by derivation of (1), i.e.

$$\mathbf{u}_{\Gamma_e, m} = \mathbf{u}_{\Gamma_e, m}^q + \mathbf{K} \mathbf{p}_{, m} + \mathbf{K}_m \mathbf{p} \quad (19)$$

where, m denotes the partial derivative with respect to a design variable z_m . \mathbf{K} and \mathbf{p} are known in advance, whereas $\mathbf{u}_{\Gamma_e, m}^q$, $\mathbf{K}_{, m}$ and $\mathbf{p}_{, m}$ have to be evaluated; $\mathbf{u}_{\Gamma_e, m}^q$ and $\mathbf{K}_{, m}$ are computed by implicit differentiation of (6), (7) and (8), and $\mathbf{p}_{, m}$ is obtained by solving another LCP.

3.1

Linear complementarity problem

At each step of the identification process, the direct problem is solved first; therefore, displacements and tractions on the external boundary, pressures \mathbf{p} and relative normal displacements \mathbf{w} along the crack are known. Then, the design sensitivities are computed.

Differentiation of (2a) with respect to a design variable, gives

$$\mathbf{w}_{, m} = \mathbf{w}_{q, m} + \mathbf{V}_{, m} \mathbf{p} + \mathbf{V} \mathbf{p}_{, m} = \mathbf{Y}_{, m} + \mathbf{V} \mathbf{p}_{, m} \quad (20)$$

with the following three possibilities for each crack node

$$\mathbf{p} = 0 \quad \mathbf{w} > 0 \implies \mathbf{w}_{, m} \neq 0 \quad \text{and} \quad \mathbf{p}_{, m} = 0 \quad (21a)$$

$$\mathbf{p} > 0 \quad \mathbf{w} = 0 \implies \mathbf{w}_{, m} = 0 \quad \text{and} \quad \mathbf{p}_{, m} \neq 0 \quad (21b)$$

$$\mathbf{p} = 0 \quad \mathbf{w} = 0 \implies \mathbf{w}_{, m} \geq 0 \quad \text{or} \quad \mathbf{p}_{, m} \geq 0 \quad (21c)$$

By means of a static condensation of the zero and sign-free sensitivities of the contact pressures, the LCP can be formulated only in terms of the pressure sensitivities $\mathbf{p}_{, m}$ referred to the nodes of the crack in contact but with zero contact pressures (Alessandri and Tralli 1995), i.e.

$$\mathbf{w}_{, m} = \mathbf{Y}_{, m} + \mathbf{V} \mathbf{p}_{, m} \geq 0 \quad (22a)$$

$$\mathbf{p}_{, m} \geq 0 \quad \mathbf{w}_{, m}^T \mathbf{p}_{, m} = 0 \quad (22b)$$

Vector $\mathbf{w}_{q, m}$ and matrix $\mathbf{V}_{, m}$ are evaluated by performing $\text{NC} + 1$ times the implicit differentiation of the DBEM. The boundary conditions are provided by the differentiation of the boundary conditions of the direct problem, i.e.

$$\mathbf{u}_{, m} = 0 \quad \text{or} \quad \mathbf{t}_{, m} = 0 \quad \text{on} \quad \Gamma_e \quad (23a)$$

$$\mathbf{t}_{, m} = 0 \quad \text{on} \quad \Gamma_c \quad (23b)$$

3.2

Boundary integral equations

In order to evaluate $\mathbf{w}_{q, m}$, $\mathbf{V}_{, m}$ and $\mathbf{u}_{\Gamma_e, m}^q$, $\mathbf{K}_{, m}$, it is necessary to differentiate Eqs. (6)–(8). The differentiation of the discretised displacement equations (6), (7) gives

$$\begin{aligned}
& c_{ij,m}(\bar{\xi})u_j(\bar{\xi}) + c_{ij}(\bar{\xi})u_{j,m}(\bar{\xi}) \\
& + \sum_{l=1}^{\text{EL}} \sum_{n=1}^2 u_{j,m}^n \int_{-1}^{+1} T_{ij}(\bar{\xi}, \mathbf{x}(\zeta))M^n(\zeta)J^l(\zeta)d\zeta \\
& - \sum_{l=1}^{\text{EL}} \sum_{n=1}^2 t_{j,m}^n \int_{-1}^{+1} U_{ij}(\bar{\xi}, \mathbf{x}(\zeta))M^n(\zeta)J^l(\zeta)d\zeta \\
& = \sum_{l=1}^{\text{EL}} \sum_{n=1}^2 t_j^n \int_{-1}^{+1} U_{ij,m}(\bar{\xi}, \mathbf{x}(\zeta))M^n(\zeta)J^l(\zeta)d\zeta \\
& + \sum_{l=1}^{\text{EL}} \sum_{n=1}^2 t_j^n \int_{-1}^{+1} U_{ij}(\bar{\xi}, \mathbf{x}(\zeta))M^n(\zeta)J_{,m}^l(\zeta)d\zeta \\
& - \sum_{l=1}^{\text{EL}} \sum_{n=1}^2 u_j^n \int_{-1}^{+1} T_{ij,m}(\bar{\xi}, \mathbf{x}(\zeta))M^n(\zeta)J^l(\zeta)d\zeta \\
& - \sum_{l=1}^{\text{EL}} \sum_{n=1}^2 u_j^n \int_{-1}^{+1} T_{ij}(\bar{\xi}, \mathbf{x}(\zeta))M^n(\zeta)J_{,m}^l(\zeta)d\zeta
\end{aligned} \tag{24}$$

$$\begin{aligned}
& \frac{1}{2}u_{i,m}(\bar{\xi}') + \frac{1}{2}u_{i,m}(\bar{\xi}'') \\
& + \sum_{l=1}^{\text{EL}} \sum_{n=1}^2 u_{j,m}^n \int_{-1}^{+1} T_{ij}(\bar{\xi}', \mathbf{x}(\zeta))M^n(\zeta)J^l(\zeta)d\zeta \\
& - \sum_{l=1}^{\text{EL}} \sum_{n=1}^2 t_{j,m}^n \int_{-1}^{+1} U_{ij}(\bar{\xi}', \mathbf{x}(\zeta))M^n(\zeta)J^l(\zeta)d\zeta \\
& = \sum_{l=1}^{\text{EL}} \sum_{n=1}^2 t_j^n \int_{-1}^{+1} U_{ij,m}(\bar{\xi}', \mathbf{x}(\zeta))M^n(\zeta)J^l(\zeta)d\zeta \\
& + \sum_{l=1}^{\text{EL}} \sum_{n=1}^2 t_j^n \int_{-1}^{+1} U_{ij}(\bar{\xi}', \mathbf{x}(\zeta))M^n(\zeta)J_{,m}^l(\zeta)d\zeta \\
& - \sum_{l=1}^{\text{EL}} \sum_{n=1}^2 u_j^n \int_{-1}^{+1} T_{ij,m}(\bar{\xi}', \mathbf{x}(\zeta))M^n(\zeta)J^l(\zeta)d\zeta \\
& - \sum_{l=1}^{\text{EL}} \sum_{n=1}^2 u_j^n \int_{-1}^{+1} T_{ij}(\bar{\xi}', \mathbf{x}(\zeta))M^n(\zeta)J_{,m}^l(\zeta)d\zeta
\end{aligned} \tag{25}$$

while the differentiation of the discretised traction equation gives

$$\begin{aligned}
& \frac{1}{2}t_{i,m}(\bar{\xi}'') - \frac{1}{2}t_{i,m}(\bar{\xi}') + n_j(\bar{\xi}'') \\
& \times \sum_{l=1}^{\text{EL}} \sum_{n=1}^2 u_{k,m}^n \int_{-1}^{+1} S_{kij}(\bar{\xi}'', \mathbf{x}(\zeta))M^n(\zeta)J^l(\zeta)d\zeta \\
& - n_j(\bar{\xi}'') \sum_{l=1}^{\text{EL}} \sum_{n=1}^2 t_{k,m}^n \int_{-1}^{+1} D_{kij}(\bar{\xi}'', \mathbf{x}(\zeta))M^n(\zeta)J^l(\zeta)d\zeta \\
& = n_{j,m}(\bar{\xi}'') \sum_{l=1}^{\text{EL}} \sum_{n=1}^2 t_k^n \int_{-1}^{+1} D_{kij}(\bar{\xi}'', \mathbf{x}(\zeta))M^n(\zeta)J^l(\zeta)d\zeta \\
& + n_j(\bar{\xi}'') \sum_{l=1}^{\text{EL}} \sum_{n=1}^2 t_k^n \int_{-1}^{+1} D_{kij,m}(\bar{\xi}'', \mathbf{x}(\zeta))M^n(\zeta)J^l(\zeta)d\zeta
\end{aligned}$$

$$\begin{aligned}
& + n_j(\bar{\xi}'') \sum_{l=1}^{\text{EL}} \sum_{n=1}^2 t_k^n \int_{-1}^{+1} D_{kij}(\bar{\xi}'', \mathbf{x}(\zeta))M^n(\zeta)J_{,m}^l(\zeta)d\zeta \\
& - n_{j,m}(\bar{\xi}'') \sum_{l=1}^{\text{EL}} \sum_{n=1}^2 u_k^n \int_{-1}^{+1} S_{kij}(\bar{\xi}'', \mathbf{x}(\zeta))M^n(\zeta)J^l(\zeta)d\zeta \\
& - n_j(\bar{\xi}'') \sum_{l=1}^{\text{EL}} \sum_{n=1}^2 u_k^n \int_{-1}^{+1} S_{kij,m}(\bar{\xi}'', \mathbf{x}(\zeta))M^n(\zeta)J^l(\zeta)d\zeta \\
& - n_j(\bar{\xi}'') \sum_{l=1}^{\text{EL}} \sum_{n=1}^2 u_k^n \int_{-1}^{+1} S_{kij}(\bar{\xi}'', \mathbf{x}(\zeta))M^n(\zeta)J_{,m}^l(\zeta)d\zeta
\end{aligned} \tag{26}$$

It is worth noting that $c_{ij,m}(\xi) = 0$ for every $\xi \in \Gamma$, $U_{ij,m} = 0 = T_{ij,m}$ for every $\xi, \mathbf{x} \in \Gamma_e$ and $J_{,m}^l = 0$ for every $\mathbf{x} \in \Gamma_e$.

The above equations can be written in matrix form as

$$\begin{aligned}
& \begin{pmatrix} H_{\Gamma_e \Gamma_e} & H_{\Gamma_e \Gamma_e^+} & H_{\Gamma_e \Gamma_e^-} \\ H_{\Gamma_e^+ \Gamma_e} & H_{\Gamma_e^+ \Gamma_e^+} & H_{\Gamma_e^+ \Gamma_e^-} \\ H_{\Gamma_e^- \Gamma_e} & H_{\Gamma_e^- \Gamma_e^+} & H_{\Gamma_e^- \Gamma_e^-} \end{pmatrix} \begin{pmatrix} \mathbf{u}_{\Gamma_e, m} \\ \mathbf{u}_{\Gamma_e^+, m} \\ \mathbf{u}_{\Gamma_e^-, m} \end{pmatrix} \\
& - \begin{pmatrix} G_{\Gamma_e \Gamma_e} & G_{\Gamma_e \Gamma_e^+} & G_{\Gamma_e \Gamma_e^-} \\ G_{\Gamma_e^+ \Gamma_e} & G_{\Gamma_e^+ \Gamma_e^+} & G_{\Gamma_e^+ \Gamma_e^-} \\ G_{\Gamma_e^- \Gamma_e} & G_{\Gamma_e^- \Gamma_e^+} & G_{\Gamma_e^- \Gamma_e^-} \end{pmatrix} \begin{pmatrix} \mathbf{t}_{\Gamma_e, m} \\ \mathbf{t}_{\Gamma_e^+, m} \\ \mathbf{t}_{\Gamma_e^-, m} \end{pmatrix} \\
& = \begin{pmatrix} 0 & H_{\Gamma_e \Gamma_e^+, m} & H_{\Gamma_e \Gamma_e^-, m} \\ H_{\Gamma_e^+ \Gamma_e, m} & H_{\Gamma_e^+ \Gamma_e^+, m} & H_{\Gamma_e^+ \Gamma_e^-, m} \\ H_{\Gamma_e^- \Gamma_e, m} & H_{\Gamma_e^- \Gamma_e^+, m} & H_{\Gamma_e^- \Gamma_e^-, m} \end{pmatrix} \begin{pmatrix} \mathbf{u}_{\Gamma_e} \\ \mathbf{u}_{\Gamma_e^+} \\ \mathbf{u}_{\Gamma_e^-} \end{pmatrix} \\
& - \begin{pmatrix} 0 & G_{\Gamma_e \Gamma_e^+, m} & G_{\Gamma_e \Gamma_e^-, m} \\ G_{\Gamma_e^+ \Gamma_e, m} & G_{\Gamma_e^+ \Gamma_e^+, m} & G_{\Gamma_e^+ \Gamma_e^-, m} \\ G_{\Gamma_e^- \Gamma_e, m} & G_{\Gamma_e^- \Gamma_e^+, m} & G_{\Gamma_e^- \Gamma_e^-, m} \end{pmatrix} \begin{pmatrix} \mathbf{t}_{\Gamma_e} \\ \mathbf{t}_{\Gamma_e^+} \\ \mathbf{t}_{\Gamma_e^-} \end{pmatrix}
\end{aligned} \tag{27}$$

where $\mathbf{u} = (\mathbf{u}_{\Gamma_e}, \mathbf{u}_{\Gamma_e^+}, \mathbf{u}_{\Gamma_e^-})$ and $\mathbf{t} = (\mathbf{t}_{\Gamma_e}, \mathbf{t}_{\Gamma_e^+}, \mathbf{t}_{\Gamma_e^-})$ collect the solution of the direct problem at each iteration step. After applying (23a) and (23b), Eq. (27) can be re-written in a more compact form as

$$\mathbf{A}\mathbf{x}_m = -\mathbf{A}_m\mathbf{x} + \mathbf{b}_m \tag{28}$$

Notice that the above equation has the same left hand side matrix \mathbf{A} as Eq. (10). The LU decomposition of \mathbf{A} , obtained for the solution of the direct problem, can be saved and re-used for the solution of system (28), with a considerable reduction of the computational effort.

The system of equations (28) is solved $\text{NC} + 1$ times in order to obtain vector $\mathbf{w}_{q,m}$ and matrix $\mathbf{V}_{,m}$ and, therefore, by solving the LCP, the vector $\mathbf{p}_m \cdot \mathbf{u}_{\Gamma_e, m}^q$ and $\mathbf{K}_{,m}$ are computed together with $\mathbf{w}_{q,m}$ and $\mathbf{V}_{,m}$ respectively.

Differentiation of (6), (7) and (8) does not increase the order of singularity of the integrals involved (Kassab et al. 1994). The singular terms appear in the displacement and traction equations only when the source point belongs to one crack line.

3.2.1

Analytic integration

The crack faces are modelled as straight lines, therefore, in this work, the design variables are restricted to the co-

ordinates of the end points of one or more crack elements. For instance, the identification of a crack modelled by a single element on each crack face would require four design variables, i.e. the co-ordinates of the end points.

Both the non-singular and the singular terms of equations (25), (26) can be evaluated on the basis of the geometric derivatives (see Fig. 2)

$$x_{i,m} = \frac{1 - \bar{\eta}\eta}{2} \delta_{im}$$

$$\delta_{im} = \begin{cases} 1 & \text{if } z_m \text{ represents a change in direction } i \\ 0 & \text{otherwise} \end{cases} \quad (29)$$

where η is a local variable normalised to the distance between two consecutive design nodes (A and B in Fig. 2), $\bar{\eta}$ the value of η either in A or in B, according to the node involved by z_m .

The weakly-singular term of the Eq. (25) can be written as

$$\int_{-1}^1 (U_{ij}(\bar{\xi}', \mathbf{x}(\zeta))J_{,m}^l(\zeta) + U_{ij,m}(\bar{\xi}', \mathbf{x}(\zeta))J^l(\zeta))M^n(\zeta)d\zeta$$

$$= \frac{\bar{\eta}}{8\pi\mu(1-\nu)} (\mathbf{g}_{ij,m}^1 + \mathbf{g}_{ij,m}^2) \quad (30)$$

where

$$\mathbf{g}_{,1}^1 = \begin{pmatrix} \frac{n_2}{2}(1-4\nu+n_2^2) & \frac{n_1}{2}(1-n_2^2) \\ \frac{n_1}{2}(1-n_2^2) & \frac{n_2}{2}(3-4\nu+n_1^2) \end{pmatrix} \quad (31)$$

$$\mathbf{g}_{,1}^2 = \begin{pmatrix} (4\nu-3)\frac{n_2}{2}WI & 0 \\ 0 & (4\nu-3)\frac{n_1}{2}WI \end{pmatrix} \quad (32)$$

$$\mathbf{g}_{,2}^1 = \begin{pmatrix} \frac{n_1}{2}(4\nu-3-n_2^2) & \frac{n_2}{2}(n_1^2-1) \\ \frac{n_2}{2}(n_1^2-1) & \frac{n_1}{2}(4\nu-1-n_1^2) \end{pmatrix} \quad (33)$$

$$\mathbf{g}_{,2}^2 = \begin{pmatrix} (3-4\nu)\frac{n_1}{2}WI & 0 \\ 0 & (3-4\nu)\frac{n_2}{2}WI \end{pmatrix} \quad (34)$$

and WI was defined in Sect. 2.2.1. The singular integral in the derivative displacement equation can be simplified as (Mellings and Aliabadi 1995)

$$\int_{-1}^1 (T_{ij}(\bar{\xi}', \mathbf{x}(\zeta))J_{,m}^l(\zeta) + T_{ij,m}(\bar{\xi}', \mathbf{x}(\zeta))J^l(\zeta))M^n(\zeta)d\zeta = 0 \quad (35)$$

therefore $H_{\Gamma_c^+ \Gamma_c^+, m} = H_{\Gamma_c^+ \Gamma_c^-, m} = 0$

The term in D_{kij} and $D_{kij,m}$, necessary for the unilateral crack, can be written as

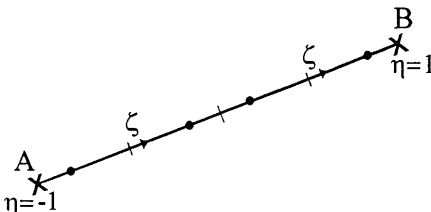


Fig. 2. Design variables

$$\int_{-1}^1 (D_{kij}(\bar{\xi}'', \mathbf{x}(\zeta))J_{,m}^l(\zeta) + D_{kij,m}(\bar{\xi}'', \mathbf{x}(\zeta))J^l(\zeta))M^n(\zeta)d\zeta$$

$$= \frac{\bar{\eta}}{6\pi L(1-\nu)} \bar{\mathbf{g}}_{kij,m} \int_{-1}^1 \frac{M^n(\zeta)}{\zeta - \zeta'} d\zeta \quad (36)$$

where

$$\bar{\mathbf{g}}_{,1} = \begin{pmatrix} -1 + 2\nu - 3n_2^2 - 6\nu n_2^2 + 10n_2^4 & n_1 n_2 (1 + 6\nu - 10n_2^2) \\ -1 - 2\nu + 9n_2^2 + 6\nu n_2^2 - 10n_2^4 & n_1 n_2 (7 - 6\nu - 10n_2^2) \\ -3 + 2\nu + 15n_2^2 - 6\nu n_2^2 - 10n_2^4 & n_1 n_2 (-3 + 6\nu - 10n_1^2) \end{pmatrix} \quad (37)$$

$$\bar{\mathbf{g}}_{,2} = \begin{pmatrix} n_1 n_2 (-3 + 6\nu - 10n_2^2) & -3 + 2\nu + 15n_1^2 - 6\nu n_1^2 - 10n_1^4 \\ n_1 n_2 (7 - 6\nu - 10n_1^2) & -1 - 2\nu + 9n_1^2 + 6\nu n_1^2 - 10n_1^4 \\ n_1 n_2 (1 + 6\nu - 10n_1^2) & -1 + 2\nu - 3n_1^2 - 6\nu n_1^2 + 10n_1^4 \end{pmatrix} \quad (38)$$

The kernel for the derivative traction equation can be written as

$$\int_{-1}^1 (S_{kij}(\bar{\xi}'', \mathbf{x}(\zeta))J_{,m}^l(\zeta) + S_{kij,m}(\bar{\xi}'', \mathbf{x}(\zeta))J^l(\zeta))M^n(\zeta)d\zeta$$

$$= \frac{2E\bar{\eta}}{9\pi L^2(1-\nu^2)} \bar{\mathbf{h}}_{kij,m} \int_{-1}^1 \frac{M^n(\zeta)}{(\zeta - \zeta')^2} d\zeta \quad (39)$$

where

$$\bar{\mathbf{h}}_{,1} = \begin{pmatrix} 2n_1 n_2 (4n_2^2 - 1) & 8n_2^4 - 8n_2^2 + 1 \\ 2n_1 n_2 (4n_1^2 - 1) & 8n_1^4 - 8n_1^2 + 1 \\ 2n_1 n_2 (4n_1^2 - 1) & -8n_1^4 + 4n_1^2 - 1 \end{pmatrix} \quad (40)$$

$$\bar{\mathbf{h}}_{,2} = \begin{pmatrix} 8n_2^4 - 4n_2^2 - 1 & 2n_1 n_2 (-4n_2^2 + 1) \\ -8n_1^4 + 8n_1^2 - 1 & 2n_1 n_2 (-4n_1^2 + 1) \\ -8n_1^4 + 8n_1^2 - 1 & 2n_1 n_2 (-4n_1^2 + 1) \end{pmatrix} \quad (41)$$

4

Flaw identification method

The identification process used is based on the knowledge of displacements at various sensor points located on the external boundary. The procedure starts with an initial guess for the shape and location of the flaw (by the design variables vector \mathbf{z}). The displacements are obtained at the sensor points by applying DBEM and solving a LCP: an error, due to the initial guess, can be computed. The design variables that minimise this error can give an approximate estimate of the actual flaw. Figure 3 shows the flowchart of the code.

If \mathbf{y}_i is the i th sensor node ($i \in (1, \dots, NS)$), $\mathbf{u}_d^{(0)}(\mathbf{y}_i)$ the measured result at this point for the d th static load ($d \in (1, \dots, D)$), $\mathbf{u}_d^{(k)}(\mathbf{y}_i)$ the computed value at the iteration k for a set $\mathbf{z}^{(k)}$, the error function is defined as

$$f(\mathbf{z}) = \frac{1}{D \times NS} \sqrt{\sum_{d=1}^D \sum_{i=1}^{NS} (\Delta_d^{(k)} \mathbf{u}(\mathbf{y}_i))^2} \quad (42)$$

where

$$\Delta_d^{(k)} \mathbf{u}(\mathbf{y}_i) = \mathbf{u}_d^{(0)}(\mathbf{y}_i) - \mathbf{u}_d^{(k)}(\mathbf{y}_i) \quad (43)$$

In order to carry out a first order minimisation technique, it is necessary to evaluate the gradient of the error function. It is given by

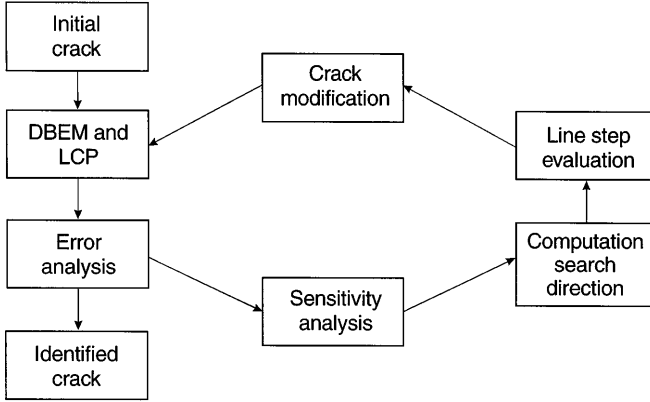


Fig. 3. Crack identification flowchart

$$(\nabla f(\mathbf{z}))_m = \frac{\partial f(\mathbf{z})}{\partial z_m} = \frac{1}{D^2 \times NS^2 \times f(\mathbf{z})} \times \sum_{d=1}^D \sum_{i=1}^{NS} \Delta_d^{(k)} \mathbf{u}(\mathbf{y}_i) \frac{\partial (\Delta_d^{(k)} \mathbf{u}(\mathbf{y}_i))}{\partial z_m} \quad (44)$$

where the terms to be calculated are

$$\frac{\partial (\Delta_d^{(k)} \mathbf{u}(\mathbf{y}_i))}{\partial z_m} = - \frac{\partial (\mathbf{u}_d^{(k)}(\mathbf{y}_i))}{\partial z_m} \quad (45)$$

5

Test examples

In this section two identification examples are considered. A plane stress plate with Young's modulus $E = 1000000$, Poisson's ratio $\nu = 0.3$ and dimensions 1×1 , all in compatible units, is considered.

The plate is supposed to have an internal unilateral frictionless crack, to be identified, with extreme points located at $(0.3, 0.5) - (0.7, 0.5)$. The DBEM allows the discretisation of the external boundary Γ_e and of the crack lines Γ_c only; therefore, it allows to avoid the subdivision of the plate in two parts at every step of the minimisation process.

Displacements at sixteen sensor points on the external boundary are supposed to be known. Fixed end boundary conditions at the lowest side of the plate are considered.

The crack is modelled by using four design variables, i.e. the co-ordinates of its extreme points.

In the first example, the upper boundary is loaded by a uniform distribution of vertical tensile traction equal to 1.0 and the extreme points of the initial guess are located at $(0.55, 0.8) - (0.8, 0.7)$. In the second example, vertical and horizontal surface tractions are applied on part of the upper side and on the lateral sides of the plate respectively, in order to have a compressive effect on the crack; the extreme points of the initial guess are located at $(0.55, 0.7) - (0.8, 0.75)$.

Figures 4–5 show the geometry, the load conditions and the crack movement during the iterative process for the two examples considered. In Fig. 5 the filled line represents the part of the crack line in contact ($\mathbf{p} > 0$) at that particular iteration step.

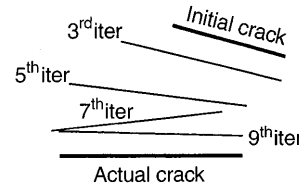
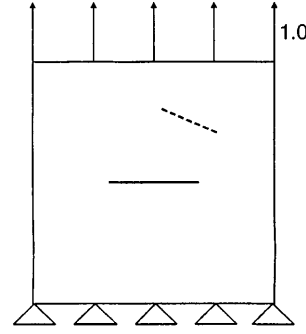


Fig. 4. Identification of a crack. First example

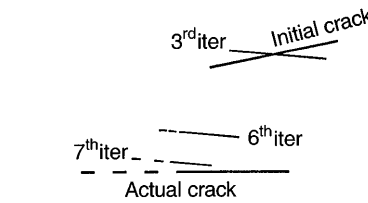
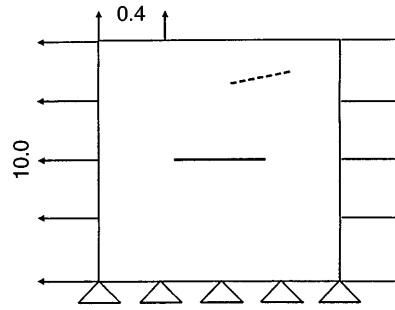


Fig. 5. Identification of a crack. Second example

Under tensile loading (first example), i.e. when no unilateral effects are activated, the procedure allows to identify correctly the position and the shape of the crack. Figures 6–7 show the convergence respectively of the normalised error and of the design variables versus the iteration step.

As for the second example, Figs. 8–9 show the normalised error and the change of the design variables versus the iteration step. This test turns out to be successful even if part of the crack is closed at many iteration steps; in this case the progressive movement of the initial crack towards its actual position is mainly due to its frictionless tangential slip deformation.

These examples confirm the considerable influence of the initial guess on the identification process. This is a quiet delicate matter in local optimisation strategies where the appearance of local minima can give wrong results. The problem occurs more frequently when unilateral effects are activated. It can be overcome by repeating the

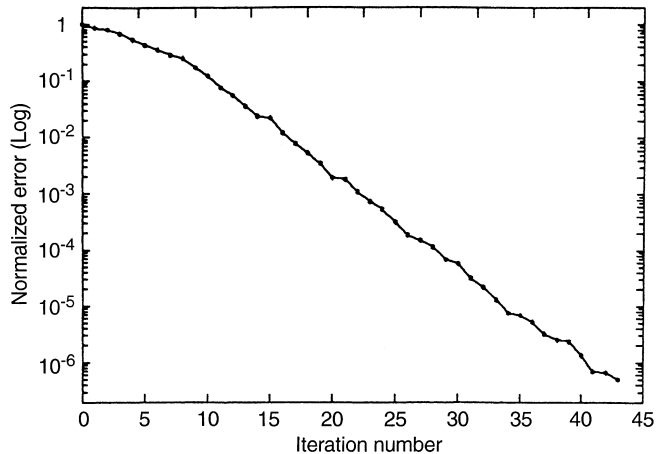


Fig. 6. Convergence of the normalised error for the open crack identification (first example)

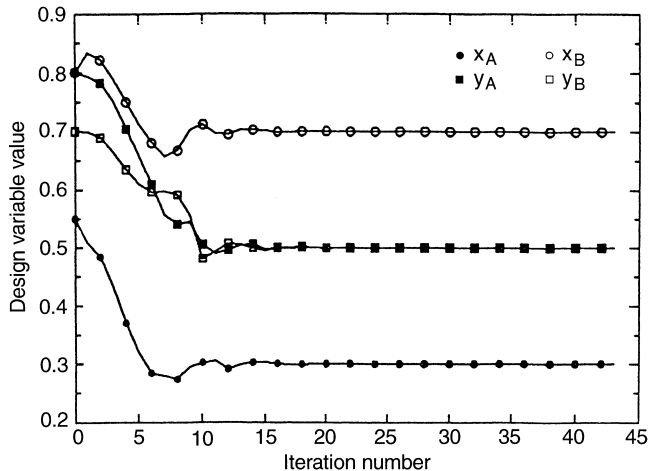


Fig. 9. Convergence of the design variables for the partially closed crack identification (second example)

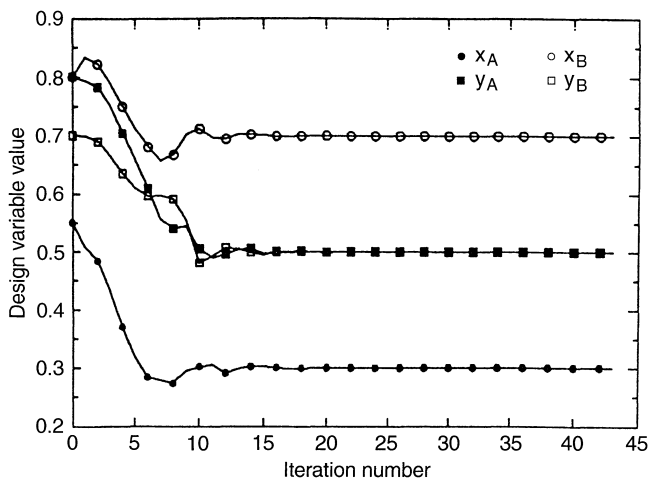


Fig. 7. Convergence of the design variables for the open crack identification (first example)

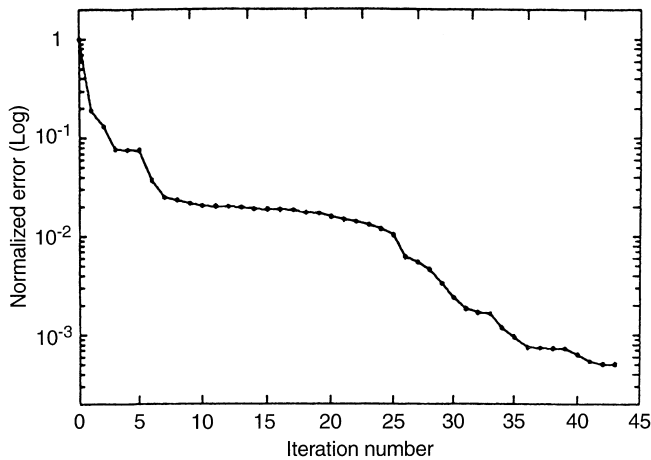


Fig. 8. Convergence of the normalised error for the partially closed crack identification (second example)

identification procedure with different initial cracks and with the minimum number of possible design variables. The process can be refined by taking as initial guess the result of the previous optimisation path.

6 Conclusions

The results obtained show that first-order nonlinear optimisation techniques, coupled with the DBEM and the LCP, can be successfully used for the solution of unilateral crack identification problems on the basis of static loading tests. The numerical procedure proposed turns out to be satisfactory with open and partially closed cracks, and it involves a relatively small number of unknowns, if compared with others. Moreover, the discretisation can be updated easily at each step of the iterative process.

The examples presented show that a flaw identification process including unilateral contact conditions on the crack surfaces can be successful. Convergence problems are out of the purpose of this paper.

Future work might include the identification of inclusions in unilateral contact with the matrix, the identification of multiple unilateral cracks and the improvement of the proposed procedure by suitable regularisation techniques.

Appendix

In the displacement equation on the crack (4), the jump terms are produced only by the integral containing the T_{ij} kernel as the internal source point approaches the boundary Γ . This integral may be written for a source point on a crack, as (see Fig. 10)

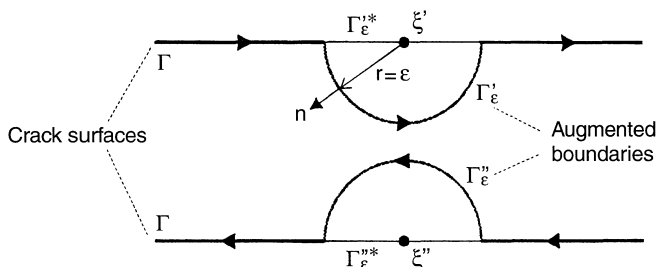


Fig. 10. The augmented boundaries on the crack faces

$$\begin{aligned}
& \int_{\Gamma} T_{ij}(\xi', \mathbf{x}) u_j(\mathbf{x}) d\Gamma(\mathbf{x}) \\
&= \lim_{\epsilon \rightarrow 0} \left\{ \int_{(\Gamma - \Gamma_{\epsilon'} - \Gamma_{\epsilon''})} T_{ij}(\xi', \mathbf{x}) u_j(\mathbf{x}) d\Gamma(\mathbf{x}) \right\} \\
&+ \lim_{\epsilon \rightarrow 0} \left\{ \int_{\Gamma_{\epsilon'}} T_{ij}(\xi', \mathbf{x}) [u_j(\mathbf{x}) - u_j(\xi')] d\Gamma(\mathbf{x}) \right\} \\
&+ u_j(\xi') \lim_{\epsilon \rightarrow 0} \left\{ \int_{\Gamma_{\epsilon'}} T_{ij}(\xi', \mathbf{x}) d\Gamma(\mathbf{x}) \right\} \\
&+ \lim_{\epsilon \rightarrow 0} \left\{ \int_{\Gamma_{\epsilon''}} T_{ij}(\xi', \mathbf{x}) [u_j(\mathbf{x}) - u_j(\xi'')] d\Gamma(\mathbf{x}) \right\} \\
&+ u_j(\xi'') \lim_{\epsilon \rightarrow 0} \left\{ \int_{\Gamma_{\epsilon''}} T_{ij}(\xi', \mathbf{x}) d\Gamma(\mathbf{x}) \right\} \\
&= I_1 + I_2 + I_3 + I_4 + I_5 \tag{46}
\end{aligned}$$

Integrals I_2 and I_4 are regular and vanish in the limiting process. The first integral I_1 can be evaluated in the Cauchy principal value sense. The integrals I_3 and I_5 can be computed analytically around the circular boundary to give the jump terms on the boundary by means of a coordinate transformation to a local system of polar coordinates and use of analytical integration

$$I_3 = \frac{1}{2} u_i(\xi') \quad I_5 = \frac{1}{2} u_i(\xi'') \tag{47}$$

The same steps can be followed for the terms involving D_{kij} and S_{kij} in the traction equation on the crack (5)

$$\begin{aligned}
& \int_{\Gamma} D_{kij}(\xi', \mathbf{x}) t_k(\mathbf{x}) d\Gamma(\mathbf{x}) \\
&= \lim_{\epsilon \rightarrow 0} \left\{ \int_{(\Gamma - \Gamma_{\epsilon'} - \Gamma_{\epsilon''})} D_{kij}(\xi', \mathbf{x}) t_k(\mathbf{x}) d\Gamma(\mathbf{x}) \right\} \\
&+ \lim_{\epsilon \rightarrow 0} \left\{ \int_{\Gamma_{\epsilon'}} D_{kij}(\xi', \mathbf{x}) n_l(\mathbf{x}) [\sigma_{kl}(\mathbf{x}) - \sigma_{kl}(\xi')] d\Gamma(\mathbf{x}) \right\} \\
&+ \sigma_{kl}(\xi') \lim_{\epsilon \rightarrow 0} \left\{ \int_{\Gamma_{\epsilon'}} D_{kij}(\xi', \mathbf{x}) n_l(\mathbf{x}) d\Gamma(\mathbf{x}) \right\} \\
&+ \lim_{\epsilon \rightarrow 0} \left\{ \int_{\Gamma_{\epsilon''}} D_{kij}(\xi', \mathbf{x}) n_l(\mathbf{x}) [\sigma_{kl}(\mathbf{x}) - \sigma_{kl}(\xi'')] d\Gamma(\mathbf{x}) \right\} \\
&+ \sigma_{kl}(\xi'') \lim_{\epsilon \rightarrow 0} \left\{ \int_{\Gamma_{\epsilon''}} D_{kij}(\xi', \mathbf{x}) n_l(\mathbf{x}) d\Gamma(\mathbf{x}) \right\} \\
&= J_1 + J_2 + J_3 + J_4 + J_5 \tag{48}
\end{aligned}$$

$$\begin{aligned}
& \int_{\Gamma} S_{kij}(\xi', \mathbf{x}) u_k(\mathbf{x}) d\Gamma(\mathbf{x}) \\
&= \lim_{\epsilon \rightarrow 0} \left\{ \int_{(\Gamma - \Gamma_{\epsilon'} - \Gamma_{\epsilon''})} S_{kij}(\xi', \mathbf{x}) u_k(\mathbf{x}) d\Gamma(\mathbf{x}) \right\} \\
&+ \lim_{\epsilon \rightarrow 0} \left\{ \int_{\Gamma_{\epsilon'}} S_{kij}(\xi', \mathbf{x}) [u_k(\mathbf{x}) - u_k(\xi')] \right. \\
&\quad \left. - u_{k,l}(\xi') (x_l - x'_l) d\Gamma(\mathbf{x}) \right\}
\end{aligned}$$

$$\begin{aligned}
& + u_k(\xi') \lim_{\epsilon \rightarrow 0} \left\{ \int_{\Gamma_{\epsilon'}} S_{kij}(\xi', \mathbf{x}) d\Gamma(\mathbf{x}) \right\} \\
&+ u_{k,l}(\xi') \lim_{\epsilon \rightarrow 0} \left\{ \int_{\Gamma_{\epsilon'}} S_{kij}(\xi', \mathbf{x}) (x_l - x'_l) d\Gamma(\mathbf{x}) \right\} \\
&+ \lim_{\epsilon \rightarrow 0} \left\{ \int_{\Gamma_{\epsilon''}} S_{kij}(\xi'', \mathbf{x}) [u_k(\mathbf{x}) - u_k(\xi'')] \right. \\
&\quad \left. - u_{k,l}(\xi'') (x_l - x''_l) d\Gamma(\mathbf{x}) \right\} \\
&+ u_k(\xi'') \lim_{\epsilon \rightarrow 0} \left\{ \int_{\Gamma_{\epsilon''}} S_{kij}(\xi'', \mathbf{x}) d\Gamma(\mathbf{x}) \right\} \\
&+ u_{k,l}(\xi'') \lim_{\epsilon \rightarrow 0} \left\{ \int_{\Gamma_{\epsilon''}} S_{kij}(\xi'', \mathbf{x}) (x_l - x''_l) d\Gamma(\mathbf{x}) \right\} \\
&= I_1 + I_2 + I_3 + I_4 + I_5 + I_6 + I_7 \tag{49}
\end{aligned}$$

In these equations, integrals J_2 , J_4 , and I_2 , I_5 are regular under basic assumptions about the continuity of the traction and displacement fields and will all vanish in the limit as $\epsilon \rightarrow 0$. The first term in the expansion of the D_{kij} integral can be evaluated in the Cauchy principal value sense, whereas the integrals I_3 and I_6 are unbounded but can be considered with the integral I_1 in the Hadamard principal value sense.

Integrals J_3 , J_5 and I_4 , I_7 can be computed analytically around the circular boundary by transformation of the coordinates into the local system. The J_3 integral is given by

$$\begin{aligned}
J_3 &= \frac{1}{16(1-\nu)} \\
&\times \begin{bmatrix} (5-4\nu)\sigma_{11}(\xi') - (1-4\nu)\sigma_{22}(\xi') & 2(1-4\nu)\sigma_{12}(\xi') \\ 2(1-4\nu)\sigma_{12}(\xi') & -(1-4\nu)\sigma_{11}(\xi') + (5-4\nu)\sigma_{22}(\xi') \end{bmatrix} \tag{50}
\end{aligned}$$

In the same way, on the opposite crack face J_5 is given by

$$\begin{aligned}
J_5 &= \frac{-1}{16(1-\nu)} \\
&\times \begin{bmatrix} (5-4\nu)\sigma_{11}(\xi'') - (1-4\nu)\sigma_{22}(\xi'') & 2(1-4\nu)\sigma_{12}(\xi'') \\ 2(1-4\nu)\sigma_{12}(\xi'') & -(1-4\nu)\sigma_{11}(\xi'') + (5-4\nu)\sigma_{22}(\xi'') \end{bmatrix} \tag{51}
\end{aligned}$$

Similarly, the terms in the S_{kij} integral expansion are

$$\begin{aligned}
I_4 &= -\frac{E}{16(1-\nu^2)} \\
&\times \begin{bmatrix} 3u_{1,1}(\xi') + u_{2,2}(\xi') & u_{1,2}(\xi') + u_{2,1}(\xi') \\ u_{1,2}(\xi') + u_{2,1}(\xi') & u_{1,1}(\xi') + 3u_{2,2}(\xi') \end{bmatrix} \tag{52}
\end{aligned}$$

$$\begin{aligned}
I_7 &= \frac{E}{16(1-\nu^2)} \\
&\times \begin{bmatrix} 3u_{1,1}(\xi'') + u_{2,2}(\xi'') & u_{1,2}(\xi'') + u_{2,1}(\xi'') \\ u_{1,2}(\xi'') + u_{2,1}(\xi'') & u_{1,1}(\xi'') + 3u_{2,2}(\xi'') \end{bmatrix} \tag{53}
\end{aligned}$$

Summing these four integrals and making use of the stress-strain relationships, the free terms on the crack are obtained

$$I_4 - J_3 = \frac{1}{2}\sigma_{ij}(\xi') \quad I_7 - J_5 = -\frac{1}{2}\sigma_{ij}(\xi'') \quad (54)$$

It must be pointed out that the rigid body condition cannot be used for Eq. (4) because the two singular terms would cancel out in the row summation as they have the same value but opposite sign.

References

- Alessandri C, Tralli A** (1995) Sensitivity analysis for unilateral contact problems: Boundary integral formulations and B.E.M. discretisations. *Comp. Mech.* 15:287–300
- Alliney S, Tralli A, Alessandri C** (1990) Boundary variational formulations and numerical solution techniques for unilateral contact problem. *Comp. Mech.* 6:247–257
- Antes H, Panagiotopoulos PD** (1992) An integral equation approach to the static and dynamic contact problems. Equality and inequality methods. Birkhäuser Verlag, Boston, Basel, Stuttgart
- Bezerra LM, Saigal S** (1993) A boundary element formulation for the inverse elastostatics problem (IESP) of flaw detection. *Int. J. Num. Meth. Eng.* 36:2189–2202
- Brebbia CA, Dominguez J** (1992) Boundary elements: an introductory course. C.M.P., Southampton, McGraw-Hill, New York
- Burczynski T, Kuhn G, Antes H, Nowakowski M** (1997) Boundary element formulation of shape sensitivity analysis for defect identification in free vibration problem. *Eng. Anal. Boundary Elem.* 19:167–175
- Cruse TA, Ewing AP, Wikswo JP** (1999) Green's function formulation of Laplace's equation for electromagnetic crack detection. *Comp. Mech.* In print
- Friedman A, Vogelius M** (1989) Determining cracks by boundary measurements. *Indiana Univ. Math. J.* 38:527–556
- Guiggiani M, Casalini P** (1987) Direct computation of Cauchy principal value integrals in advanced boundary elements. *Int. J. Num. Meth. Eng.* 24:1711–1716
- Guiggiani M, Krishnasamy TJ, Rudolph TJ, Rizzo FJ** (1992) A general algorithm for the numerical solution of hypersingular boundary integral equations. *ASME J. App. Mech.* 59:604–614
- Hong H, Chen J** (1988) Derivations of integral equations of elasticity. *J. Eng. Mech. ASCE* 114:1028–1044
- Kassab AJ, Moslehy FA, Daryapurkar AB** (1994) Nondestructive detection of cavities by an inverse elastostatic boundary element method. *Eng. Anal. Boundary Elem.* 13:45–55
- Kobayashi S** (1994) Inverse analysis by boundary element method. *Boundary Elements XVI*. In: Brebbia CA (eds), Computational Mechanics Publication, 141–148
- Liu YJ** (1998) Analysis of shell-like structures by the boundary element method based on 3-D elasticity: formulation and verification. *Int. J. Num. Meth. Eng.* 41:541–558
- Liu YJ, Zhang D, Rizzo FJ** (1993) Nearly singular and hypersingular integrals in the boundary element method. *Boundary Elements XV*. In: Brebbia CA, and Rencis JJ (eds), Computational Mechanics Publication, 453–468
- Mallardo V, Aliabadi MH** (1998) A BEM sensitivity and shape identification analysis for acoustic scattering in fluid-solid problems. *Int. J. Num. Meth. Eng.* 41:1527–1541
- Martini PA, Rizzo FJ, Cruse TA** (1998) Smoothness-relaxation strategies for singular and hypersingular integral equations. *Int. J. Num. Meth. Eng.* 42:885–906
- Mellings SC, Aliabadi MH** (1995) Flaw identification using boundary element method. *Int. J. Num. Meth. Eng.* 38:399–419
- Nishimura N, Kobayashi S** (1991) A boundary integral equation method for an inverse problem related to crack detection. *Int. J. Num. Meth. Eng.* 32:1371–1387
- Nishimura N, Kobayashi S** (1995) Crack determination in time domain with collocation BIEM. *Computational Mechanics '95*. In: Atluri SN, Yagawa G & Cruse TA (eds), Springer, Berlin, 2862–2867
- Santosa F, Vogelius M** (1991) A computational algorithm to determine cracks from electrostatic boundary measurements. *Int. J. Eng. Sci.* 29:917–937
- Schnur DS, Zabarav N** (1992) An inverse method for determining elastic material properties and a material interface. *Int. J. Num. Meth. Eng.* 33:2039–2057
- Simunovic S, Saigal S** (1992) Frictionless contact with BEM using quadratic programming. *ASCE J. Eng. mech.* 118(9):1876–1891
- Simunovic S, Saigal S** (1994) Frictional contact formulation using quadratic programming. *Comp. Mech.* 15:173–187
- Stavroulakis GE, Antes H** (1997) Nondestructive elastostatic identification of unilateral cracks through BEM and neural networks. *Comp. Mech.* 20:439–451
- Tanaka M, Masuda Y** (1986) Boundary element method applied to some inverse problems. *Eng. Anal. Boundary Elem.* 3(3):138–143
- Tanaka M, Nakamura M, Nakono T** (1992) Defect shape identification by the elastodynamic boundary element method using strain responses. *Inverse Problems in Engineering Mechanics*. In: Bui Tanaka (eds), Springer-Verlag, Iutam Symposium Tokio/Japan, 137–151
- Tosaka N, Utani A, Takahashi H** (1995) Unknown defect identification in elastic field by boundary element method with filtering procedure. *Eng. Anal. Boundary Elem.* 15:207–215
- Zeng X, Saigal S** (1992) An inverse formulation with boundary elements. *ASME J. App. Mech.* 59:835–840